

# Dynamic properties and liquefaction potential of soils

T. G. Sitharam\*, L. GovindaRaju and A. Sridharan

Department of Civil Engineering, Indian Institute of Science, Bangalore 560 012, India

**Design of geotechnical engineering problems that involve dynamic loading of soils and soil–structure interaction systems requires the determination of two important parameters, the shear modulus and the damping of the soils. The recent developments in the numerical analyses for the nonlinear dynamic responses of grounds due to strong earthquake motions have increased the demand for the dynamic soil properties corresponding to large strain level also. Further, the most common cause of ground failure during earthquakes is the liquefaction phenomenon which has produced severe damage all over the world. This paper summarizes the methods of determining the dynamic properties as well as potential for liquefaction of soils. Parameters affecting the dynamic properties and liquefaction have been brought out. A simple procedure of obtaining the dynamic properties of layered ground has been highlighted. Results of a series of cyclic triaxial tests on liquefiable sands collected from the sites close to the Sabarmati river belt have been presented.**

DURING the recent Bhuj earthquake on 26 January 2001, a number of medium to high rise residential buildings collapsed in Ahmedabad city, which is located about 300 km away from the epicenter<sup>1</sup>. The city is founded over thick recent unconsolidated sediments. The severe damages in this location are attributed to the response of such unconsolidated sediments to violent shaking. This catastrophic earthquake has provided a serious reminder that liquefaction of sandy soils and sands with non-plastic fines as a result of earthquake ground shaking poses a major threat to the safety of civil engineering structures. In order to evaluate the response of foundations subjected to vibrations and the manner of vibrations and its transmission through the ground, the dynamic characteristics of soils must be determined. Also, investigations to evaluate the liquefaction potential of soil deposits during earthquakes have been the subject of much attention in recent years.

## Measurement of dynamic soil properties

Dynamic analyses to evaluate the response of the earth structures to dynamic stress applications, such as those produced by earthquakes, blasting, wind loading or machine

vibrations, are finding increased applications in civil engineering practice. Various idealized models and analytical techniques may be used to represent a soil deposit and its response. Regardless of type of procedure, it is first necessary to evaluate the appropriate dynamic properties of the materials in the deposit. Precise measurement of dynamic soil properties is somewhat a difficult task in the solution of geotechnical earthquake engineering problems<sup>2</sup>. Several laboratory and field techniques are available to measure the dynamic properties in which many are employed in these measurements at low-strain and many are in the large strain levels. However, the choice of a particular technique depends on the specific problem to be solved. Figure 1 shows the changes in soil properties with shear strain<sup>3</sup>.

## Methods to evaluate dynamic properties of soil

### Laboratory testing

Many experimental methods have been developed from time to time. Figure 2 shows the various methods at a glance. The laboratory methods have been determined with small samples and the level of displacement is very different. However, they have the advantages of controlled testing and being economical.

*Low-strain tests.* Very few laboratory tests are available to measure the dynamic properties of soils at low strain levels. Resonant column test, ultrasonic pulse test and the piezoelectric bender element test are the commonly employed techniques. Among these methods, the resonant column method is popular. There are different versions of this method using different end conditions for the sample. Skoglund *et al.*<sup>4</sup> have compared the results obtained from

Shear Strain	10 <sup>-6</sup>	10 <sup>-5</sup>	10 <sup>-4</sup>	10 <sup>-3</sup>	10 <sup>-2</sup>	10 <sup>-1</sup>
	Small Strain	Medium Strain		Large Strain	Failure Strain	
Elastic						
Elasto-Plastic						
Failure						

**Figure 1.** Changes in soil properties with shear strain.

\*For correspondence. (e-mail: sitharam@civil.iisc.ernet.in)

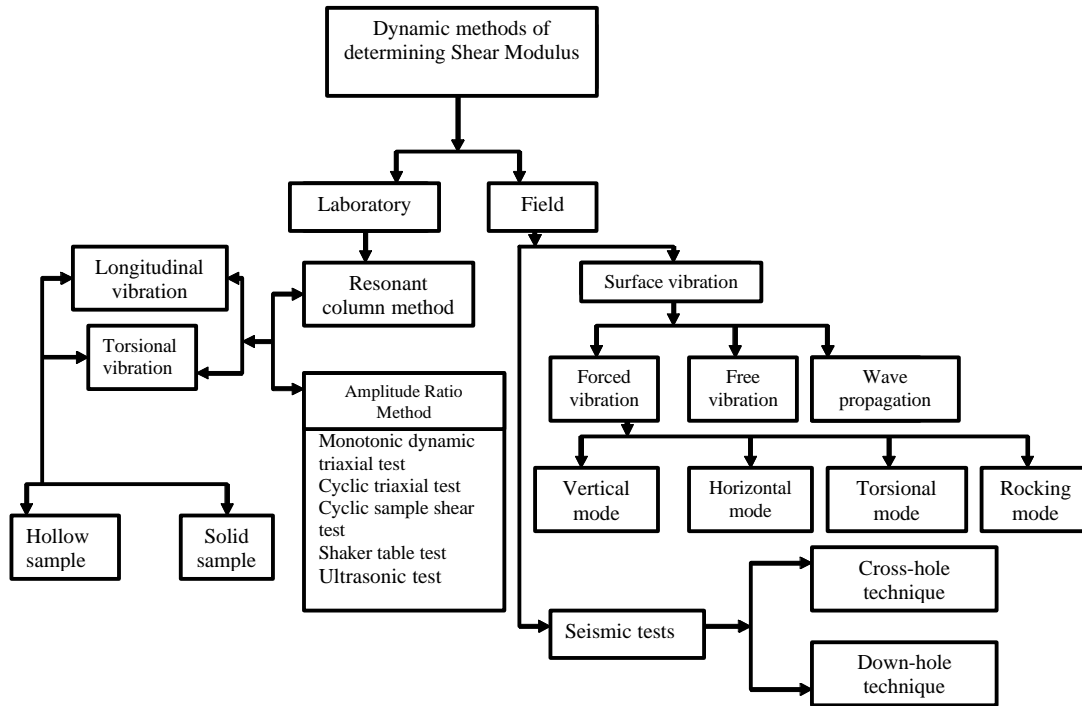


Figure 2. Classification of dynamic methods of obtaining shear modulus.

several of the resonant column devices and concluded that measured dynamic moduli from different devices were consistent.

*High-strain tests.* For the measurement of strain-dependent dynamic properties, several devices have been developed. Typical examples are cyclic triaxial test, cyclic direct simple shear test and cyclic torsional shear test devices.

*Field testing*

Evaluation of dynamic soil properties by field tests has a number of advantages, as these tests do not require sampling that can alter the stress and structural conditions in soil specimens. Further, the tests measure the response of relatively large volumes of soil. However, these field tests can be again classified based on the range of magnitude of strain as low-strain and high-strain tests.

*Low-strain field tests.* Dynamic soil properties depend much on the shear strain level. In the strain range below the order of 0.001%, the deformations shown by most of the soils are purely elastic and recoverable and the dampings are negligible. Low-strain tests operate below the strain specified above and are based on the theory of wave propagation in the materials. Some of the low-strain field tests are seismic reflection test, seismic refraction test, suspension logging test, steady-state vibration or rayleigh wave test, spectral analysis of surface wave test (SASW), seismic cross-hole test, seismic down-hole (up-hole) test and seismic cone test.

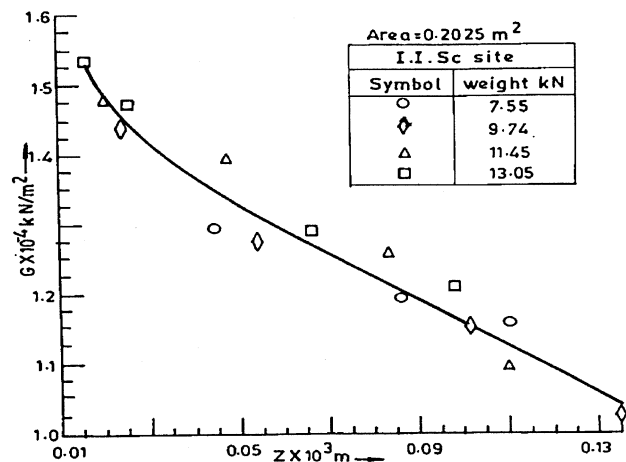


Figure 3. Resonance amplitude vs dynamic shear modulus.

*High-strain field tests.* At higher range of shear strains, the behaviour of soils is elasto-plastic and produces irrecoverable permanent deformations in the soil. Standard penetration test (SPT), Cone penetration test (CPT), Dilatometer test and pressuremeter test are of particular importance to measure high-strain characteristics of soil.

**Factors affecting the dynamic moduli of soils**

Many investigators have brought out that one of the most important parameters that affect the dynamic moduli is the displacement amplitude or strain level at which the dynamic modulus is measured. Figure 3 presents typical

results of the variation of shear modulus with respect to the displacement amplitude at resonance under different static loads for red earth of Bangalore. The shear modulus has been obtained from surface vibration tests evaluating the resonance frequency<sup>5</sup>. Similar results have been obtained for different contact areas and reported. From these results and other published data, it could be seen that the shear modulus significantly decreases with increase in displacement amplitude, bringing out the importance of the level of the displacement amplitude while determining moduli in the field. It is also brought out that the effects of static load and area of foundation on the dynamic shear modulus could be taken as marginal as long as the displacement amplitude is considered. In other words, the resonance can be taken as a single parameter influencing the dynamic modulus. Similar conclusions could be made from the analysis of the test results of Fry<sup>6</sup> for uniform fine sand and refs 7, 8 for beach sand.

Gandhi<sup>9</sup> after carrying out detailed analysis of the published results and results by him proposed a relationship between shear modulus and the displacement amplitude as

$$A_{max}/G = a_2 + b_2 A_{max} \tag{1}$$

He found for eq. (1)  $a_2 = 0.93 \times 10^{-4} \text{ cm}^3/\text{kg}$  and  $b_2 = 0.0061 \text{ cm}^2/\text{kg}$  with a high correlation coefficient of 0.937. Since the results used in these analyses belong to different soils from different places and for different static and dynamic loading conditions, eq. (1) could be used with certain amount of confidence.

### Dynamic spring constant

Sridharan and Gandhi<sup>8</sup> introduced a new method to determine what is called ‘dynamic spring constant’,  $K_A$  of a soil defined as the ratio of the dynamic load at any frequency to the corresponding amplitude. The dynamic spring constant obtained using the resonance amplitude,  $K_{Ar}$  had

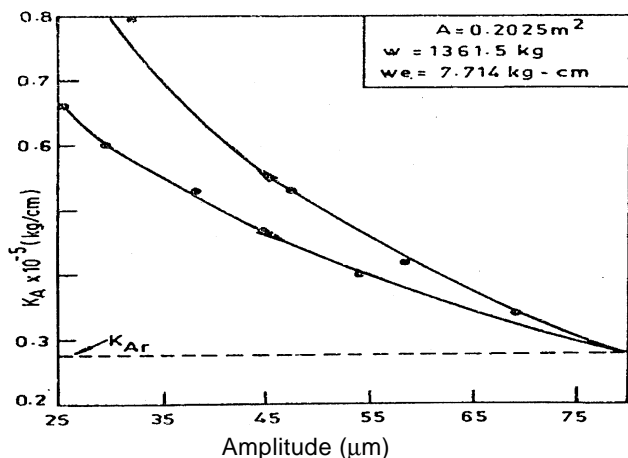


Figure 4. Amplitude vs dynamic spring constant,  $K_A$ .

been compared with spring constant from resonance frequency  $K_{fr}$  (eq. (2)). Figure 4 shows typical results of  $K_A$  obtained at different amplitude levels.

$$f_{mr} = \frac{1}{2p} \sqrt{\frac{k}{M}} \frac{1}{\sqrt{1-2D^2}} \tag{2}$$

Here  $f_{mr}$  = resonance frequency,  $k$  = spring constant,  $M$  = total static mass of the system and  $D$  = damping factor.

The same trend is reflected in the post-resonance part of the curve. The arrows show the increase and decrease of frequency. The stiffness obtained from post-resonance part is more than that of the pre-resonance part. The variation in  $K_A$  is primarily due to the variation in the amplitude.

### Layered soil systems

There are a number of instances in which the natural soil could be layered. For a layered soil system, the stiffness obtained from an idealization of soils underneath as springs in series gives the same value of stiffness irrespective of location and extent of individual soil layers with respect to the base of the foundation. A simple method called the ‘weighted average method’ has been proposed by Sridharan *et al.*<sup>10</sup> to obtain the equivalent stiffness of a layered soil system knowing their individual values, their relative position with respect to foundation base and their thickness. Figure 5 shows a typical layered system of 4 layers.

The analysis is based on Boussinesq theory and can also be used when any number of layers is present. In the analysis, the effective depth of influence is assumed to be three times the width  $B$  of the footing. In other words, the stresses almost decay to a negligible value within a depth of  $3B$ . The layer system shown in Figure 5 is further subdivided into a number of sublayers. At the centre of each sublayer the Boussinesq stress influence coefficient,  $I$  is calculated for a square footing subjected to a uniformly distributed load. The individual sublayer influence factor,  $I_j$  is obtained by dividing each of the coefficients by the sums of all the coefficients up to the depth of influence, namely  $3B$ . The equivalent stiffness of the layer system is then defined as

$$K_{eq} = \sum k_j I_j = k_1(\sum I_j)h_1 + k_2(\sum I_j)h_2 + k_3(\sum I_j)h_3 + \dots \tag{3}$$

The values of  $I_j$  cumulatively added up from zero thickness to maximum thickness give rise to a factor  $\sum I_j$  which can also be used to obtain the equivalent stiffness. Figure 6 shows the variation of  $\sum I_j$  with respect to the ratio of thickness,  $h$  to the width,  $B$  of the footing.

The above theoretical formulations have been examined with experimental results. Their results clearly indicate that the top layer material will primarily control the overall behaviour if the top layer thickness is more than  $2B$ . The equivalent spring constant was calculated using the weigh-

ted average method and Odemark<sup>11</sup> method. Figure 7 presents some typical results of comparison between the two theories and experiments.

**Factors controlling liquefaction**

Many factors govern the liquefaction process for *in situ* soil and the most important are intensity of earthquake and its duration, location of ground water table, soil type, soil relative density, particle size gradation, particle shape, depositional environment of soil, soil drainage conditions, confining pressures, aging and cementation of the soil deposits, historical environment of the soil deposit and building/

additional loads on these deposits. In summary, the site conditions and soil type that are most susceptible to liquefaction are given in the following sections.

*Site conditions*

The site that is close to the epicenter of fault rupture of a major earthquake. A site that has a ground water table close to ground surface.

*Soil type most susceptible to liquefaction for given site conditions*

Sand that has uniform gradation and rounded particles, very loose density state, recently deposited with no cementation between soil grains, and no prior preloading or seismic shaking.

**Methods to evaluate liquefaction potential of soil**

Several approaches to evaluate the potential for liquefaction have been developed. The commonly employed methods are cyclic stress approach and cyclic strain approach to characterize the liquefaction resistance of soils both by laboratory and field tests. The cyclic stress approach to evaluate liquefaction potential characterizes both earthquake loading and the soil liquefaction resistance in terms of cyclic stresses. But, in the cyclic strain approach, earthquake loading and liquefaction resistance are characterized by cyclic strains. Cyclic triaxial test, cyclic simple shear test and cyclic torsional shear test are the common laboratory tests. Further, Standard Penetration Test, Cone Penetration Test, Shear wave velocity method, Dilatometer test are some of the *in situ* tests to characterize the liquefaction resistance. Even though cyclic stress and cyclic strain approaches are most widely used in the field of geotechnical earthquake engineering, some other approaches such as energy dissipation, effective stress based response analysis and probabilistic approaches have been also developed. Figure 8 presents a chart<sup>12</sup> that can be employed to determine the cyclic resistance ratio of the *in situ* soil. This chart was developed from observations and investigations of numerous sites that had liquefied and did not liquefy during the earthquakes.

Figures 9 and 10 can be used to evaluate the cyclic resistance ratio of *in situ* soil using cone penetration test data for clean sands and silty sands and clean gravels and silty gravels<sup>13</sup> respectively. This method is an alternative to standard penetration test in which the corrected CPT tip resistance  $q_{c1}$  is used.

Figure 11 presents a chart for evaluating the liquefaction resistance of the *in situ* soil based on the measured shear wave velocity of the soil<sup>14</sup>. The shear wave velocity can be measured *in situ* employing different geophysical techni-

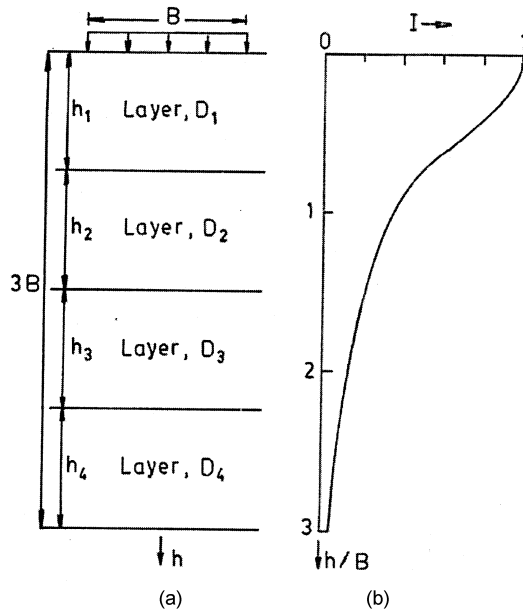


Figure 5. Layered soil system of four layers.

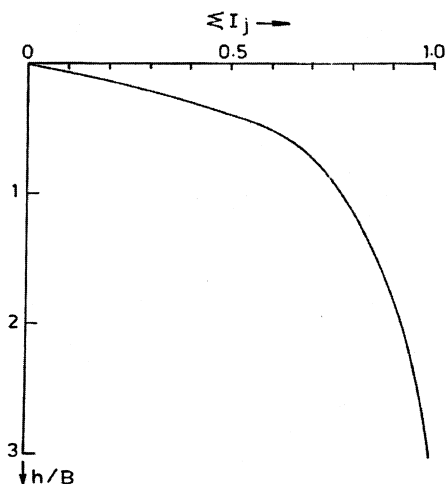


Figure 6. Variation of influence factor with respect to the ratio of thickness  $h$  to the width  $B$  of footing.

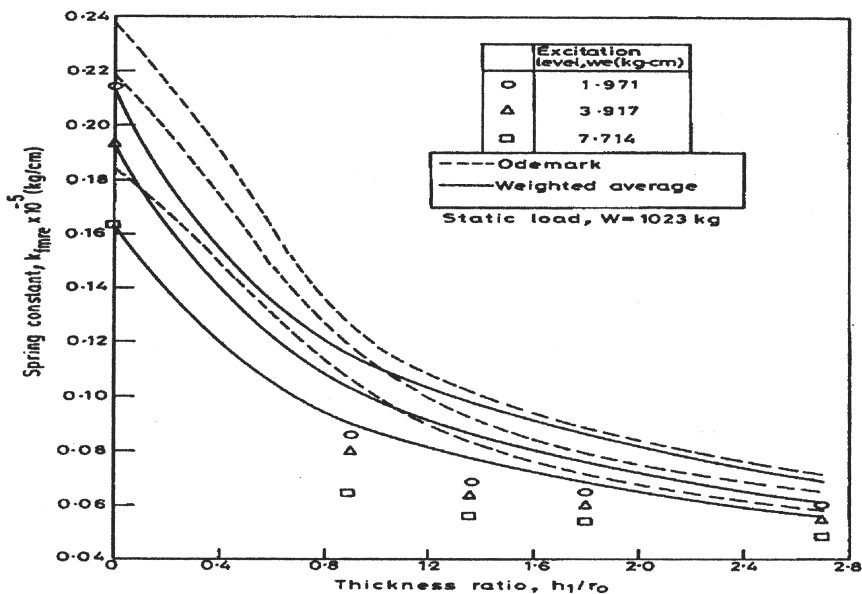


Figure 7. Variation of equivalent spring constant with thickness of saw dust as top layer in 3-layered system.

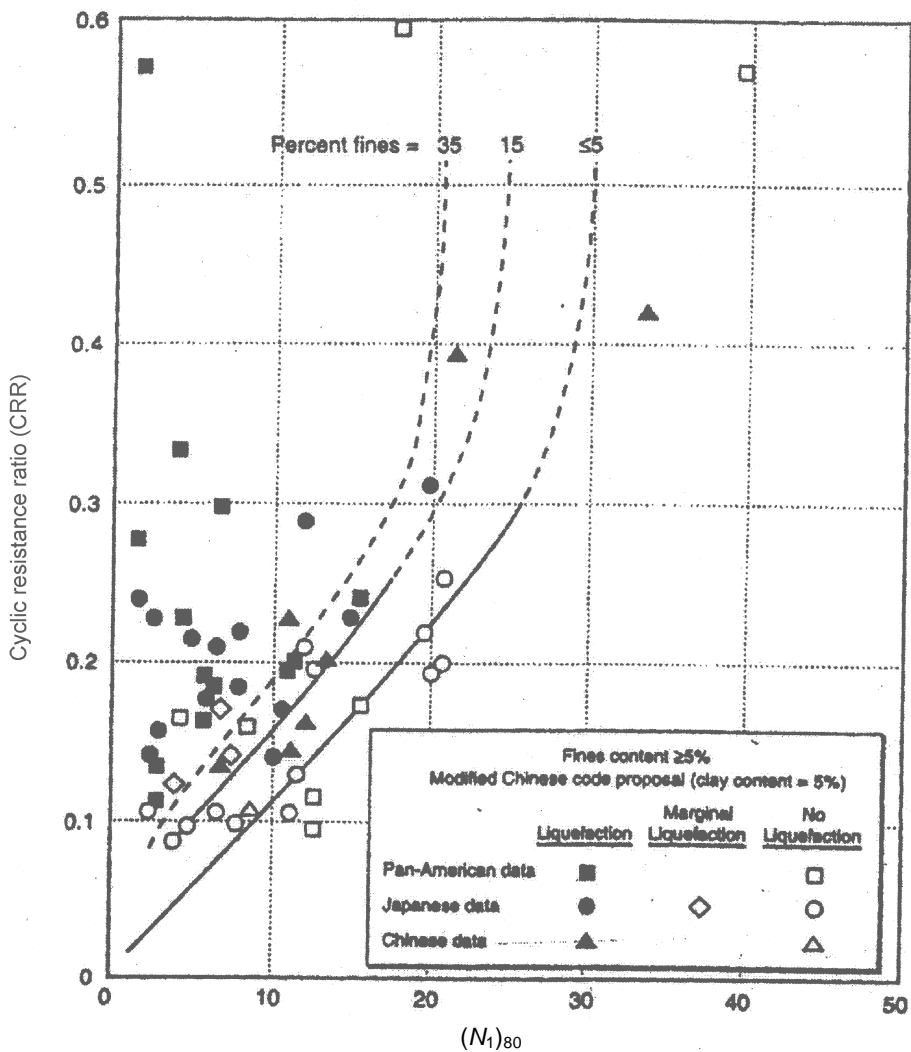


Figure 8. Cyclic resistance ratio causing liquefaction and  $(N_1)_{80}$  values for magnitude 7.5 earthquake for clean sands and silty sands<sup>12</sup>.

ques, such as the uphole, down-hole, or cross-hole methods. Here,  $v_{s1}$  represents the corrected shear wave velocity.

**Evaluation of dynamic properties and liquefaction potential of soils**

*Soil sampling and characterization*

Soil samples were collected from the locations close to the right bank of Sabarmati river belt in Ahmedabad where

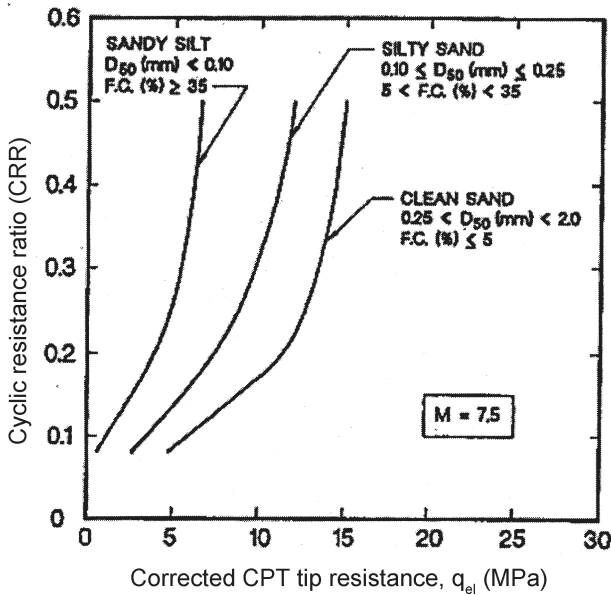


Figure 9. Cyclic resistance ratio causing liquefaction and corrected CPT tip resistance values for magnitude 7.5 earthquake for clean sand, silty sands and sandy silt<sup>13</sup>.

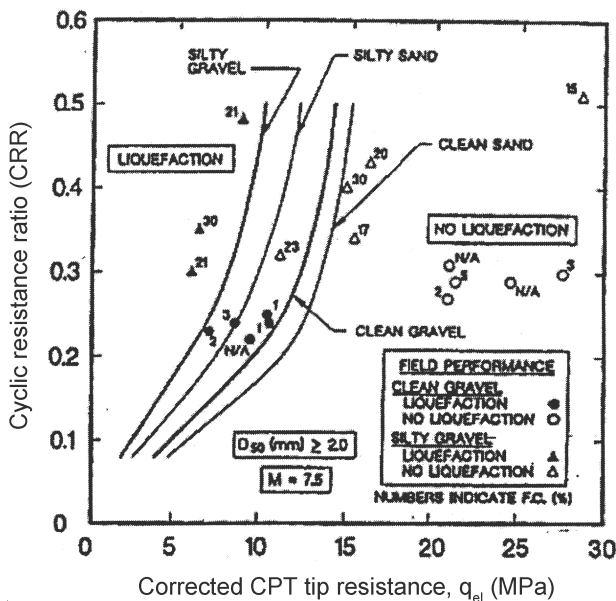


Figure 10. Cyclic resistance ratio (CRR) and corrected CPT tip resistance values for magnitude 7.5 earthquake for clean gravel and silty gravel<sup>13</sup>.

extensive damage to the constructed facilities was observed during Bhuj earthquake. Table 1 gives the summary of the index properties of the soil sample collected. Figure 12 shows the ranges of grain size distribution for liquefaction susceptible soils proposed by Tsuchida<sup>15</sup>. Also shown in this figure is the grain size distribution of the soil sample, which is most liquefiable.

**Experimental investigation**

*Sample preparation*

Many of the water sedimentation depositional methods tend to produce inhomogeneous specimens with the coarser fraction on the bottom and the finer fraction on the top of the specimen<sup>16</sup>. Dry pluviation has been shown to create a grain structure similar to that of naturally deposited river sands. In view of these observations, dry pluviation method was employed in the present study to prepare the soil samples. Cylindrical soil specimens of size 50 mm diameter and 100 mm height were prepared by placing the dry silty sand in a funnel with a tube attached to the spout.

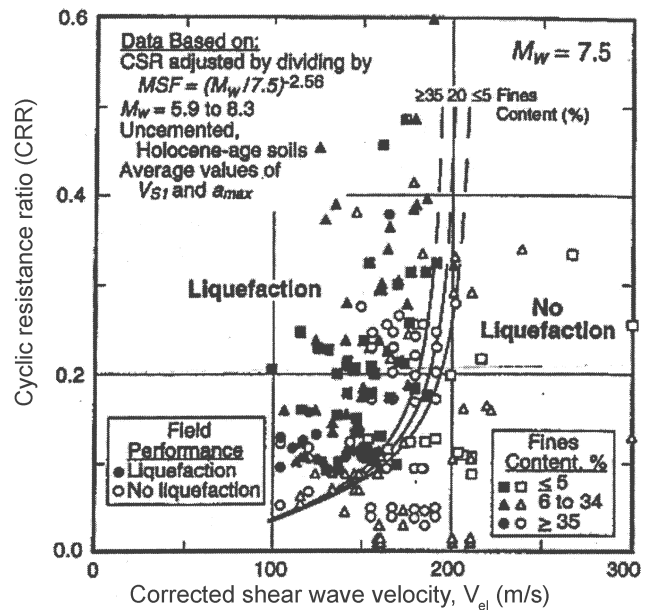


Figure 11. Cyclic resistance ratio (CRR) causing liquefaction and shear wave velocity for clean sand, silty sand and sandy silt<sup>14</sup>.

Table 1. Index properties of soil

Specific gravity	2.66
Medium sand	37%
Fine sand	53.4%
Silt content	9.6%
Clay content	-
Maximum void ratio	0.67
Minimum void ratio	0.54

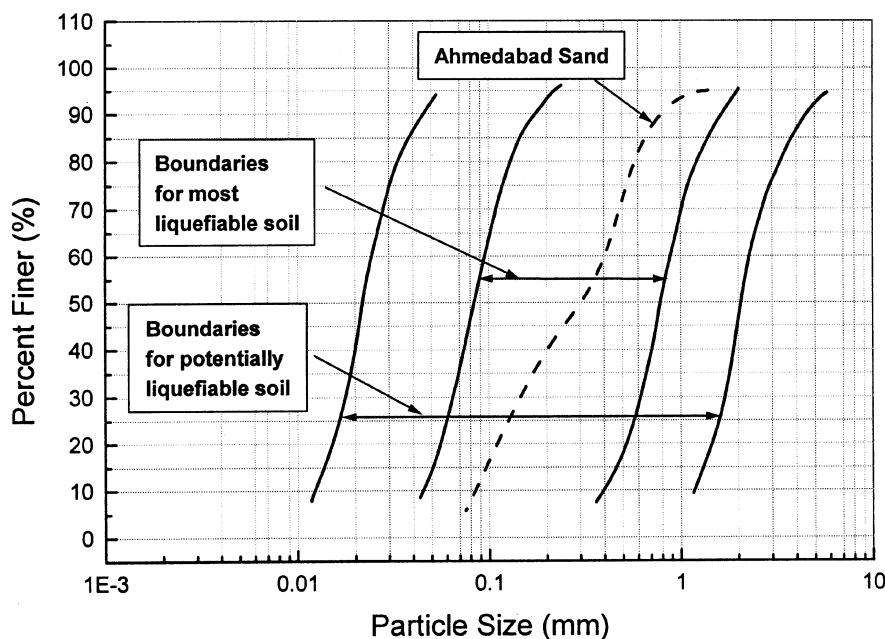


Figure 12. Ranges of grain size distribution for liquefaction susceptible soils.

The tube was placed at the bottom of the membrane lined split mould. The tube was slowly raised along the axis of symmetry of the specimen, such that the soil was not allowed any drop in height. This procedure was used to achieve the loosest possible density for a specimen prepared in a dry state. While preparing the soil specimens at relatively higher densities, the mould was gently tapped in a symmetrical pattern until the desired density was achieved. Using the above technique, soil specimens with two different target initial relative densities (RD) of 30% and 70% were prepared. After the specimens were prepared, a small vacuum pressure of 10 kPa was applied to the specimens to reduce disturbance during the removal of split mould and triaxial cell installation. The specimens were then saturated with deaired water using backpressure saturation. Saturation of the specimens was checked by measuring Skempton’s pore pressure parameter B. Following the saturation, the specimens were then isotropically consolidated to the required confining pressure.

*Cyclic loading and data acquisition*

Strain-controlled cyclic triaxial tests were carried out on isotropically consolidated soil specimens under undrained conditions to simulate essentially undrained field conditions during earthquake<sup>17</sup>. Cyclic loading was applied on the specimens using hydraulic actuator. The tests were conducted at a constant cyclic axial strain of varying magnitudes. In the entire test program, a frequency of 1 Hz with sinusoidal wave and an effective confining pressure of 100 kPa were maintained. The axial deformation, cell

pressure, cyclic load and pore water pressure were monitored using a built-in data acquisition system.

**Results**

*Evaluation of dynamic properties of soil*

*Data calculation.* When cyclic triaxial tests are performed on soil specimen, a hysteresis loop similar to the one shown in Figure 13 will be formed in the plot of deviator stress,  $s_d$ , versus axial strain,  $e$ . The slope of the secant line connecting the extreme points on the hysteresis loop is the dynamic Young’s modulus,  $E$ , which is given by

$$E = s_d / e. \tag{4}$$

Further,

$$g = (1 + n) e \quad \text{and} \quad G = E/2 (1 + n), \tag{5}$$

where  $G$  is the shear modulus,  $g$  is the shear strain and  $n$  is the Poisson’s ratio that may be taken as 0.5 for saturated undrained specimens<sup>18</sup>. The damping ratio,  $D$ , is a measure of dissipated energy versus elastic strain energy, and may be computed from the equation

$$D = \frac{1}{4p} \frac{A_L}{A_T}, \tag{6}$$

where  $A_L$  = area enclosed by the hysteresis loop; and  $A_T$  = area of the shaded triangle.

The effect of relative density (void ratio) on the dynamic properties of saturated sand is examined with two differ-

ent relative densities for the same confining pressure of 100 kPa. Figures 14 and 15 show the variation of shear modulus and damping as a function of shear strain for Ahmedabad sand. It is clear that the reduction in shear modulus and increase in damping vary significantly over a range of shear strains tested (0.053% to 5%). The soil, which is initially stiff, loses its stiffness due to the increase in pore water pressure as number of the loading cycles increase. The progression of loading cycles induces higher magnitudes of pore water pressures resulting in drastic reduction of shear modulus. The soil samples with higher relative densities exhibit slightly higher shear modulus in the range of shear strain 0.053% to 0.5%. But, more or less the same values of shear modulus occur beyond 0.5% shear strain level irrespective of the initial density of the

soil. The scatter in the values of shear modulus and damping of soil for the relative densities of 30% and 70% fall in the narrow band in the range of shear strains tested.

*Evaluation of liquefaction potential of soil*

Figure 16 shows a plot of variation of deviator stress and pore pressure ratio with number of cycles for the soil at

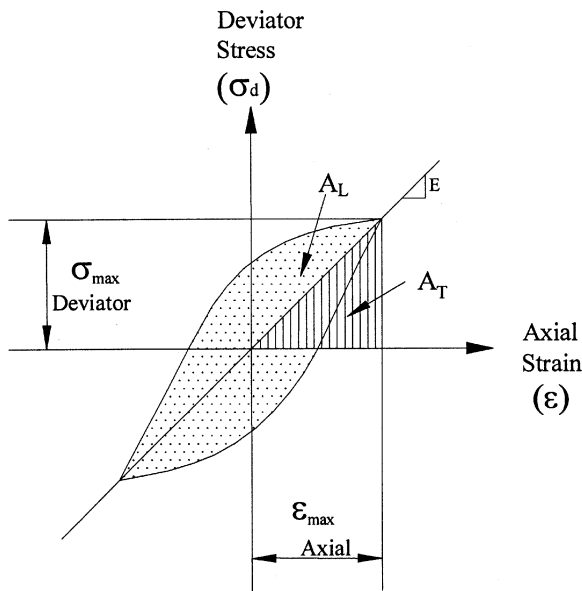


Figure 13. Hysteretic stress-strain relationship for cyclic loading.

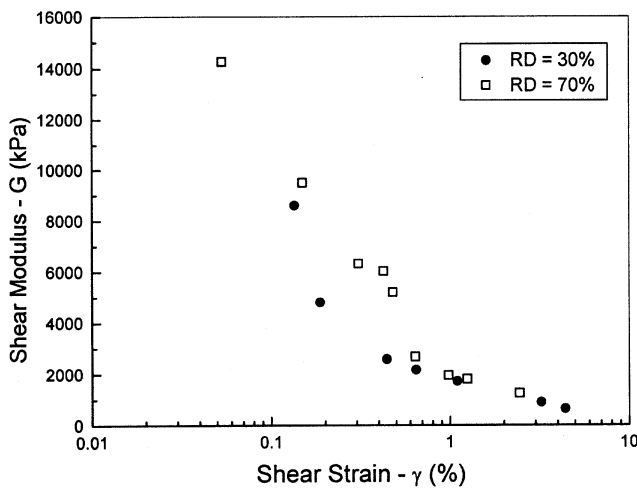


Figure 14. Variation of shear modulus with shear strain.

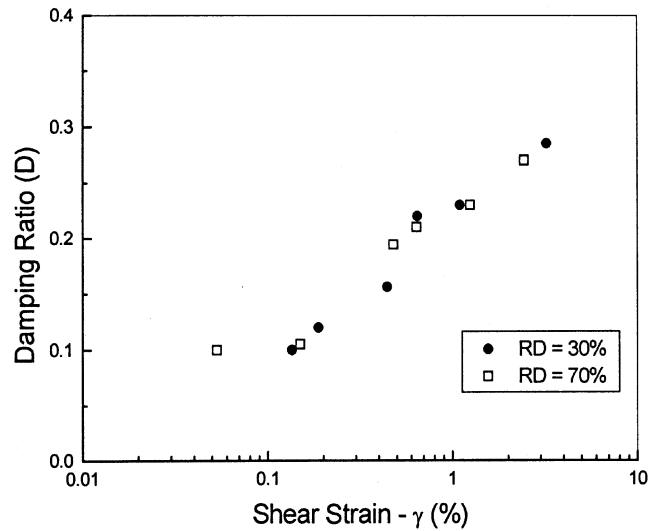


Figure 15. Variation of damping ratio with shear strain.

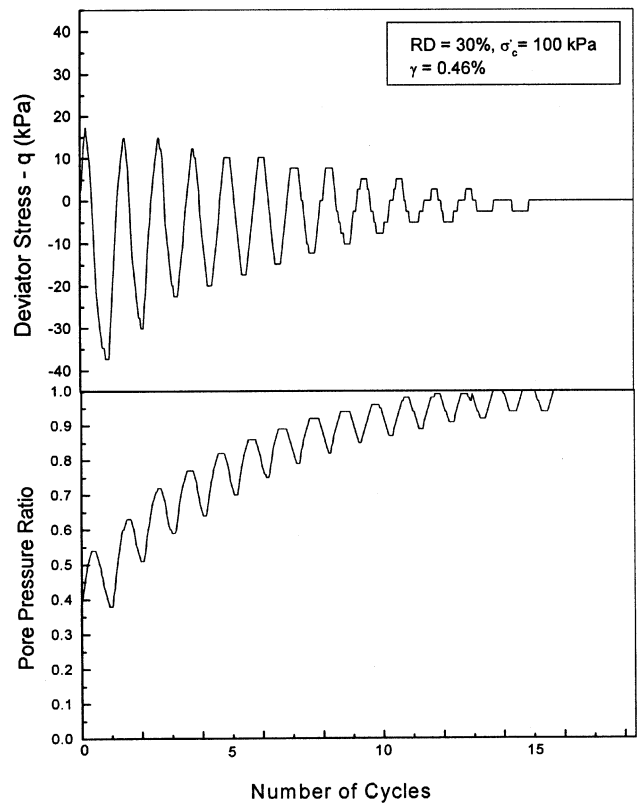


Figure 16. Variation of deviator stress and pore pressure ratio with number of cycles.

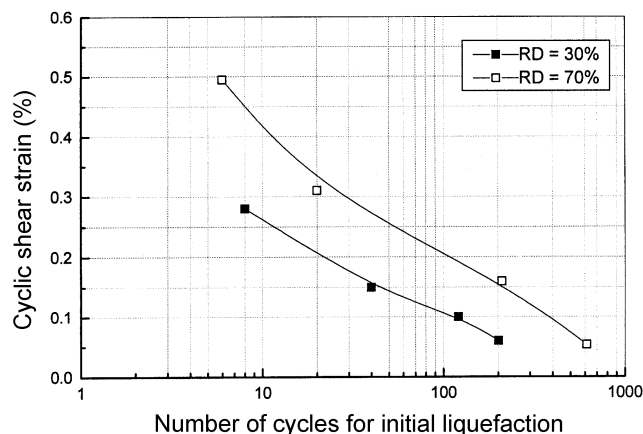


Figure 17. Cyclic resistance curves.

an initial relative density of 30% tested at constant cyclic shear strain (single amplitude) of 0.46% in strain-controlled cyclic test. It is evident that the pore water pressure builds up steadily as the cyclic shear strain is applied, and eventually approaches a value equal to the initially applied confining pressure of 100 kPa (cyclic pore pressure ratio = 100%) in 14 cycles of loading. The increase in pore water pressure results in a corresponding decrease in the effective stress, which finally reduces to zero when the pore water pressure ratio is equal to 100%. Such a state of the specimen is recognized as 'liquefaction' which is a state of softening produced suddenly with the complete loss of shear strength or stiffness. Figure 17 represents the cyclic resistance in terms of cyclic shear strain (single amplitude) vs number of cycles for initial liquefaction for different relative densities (RD).

### Concluding remarks

Dynamic properties play a vital role in the design of structures subjected to dynamic loads. A simple method to obtain the equivalent modulus of layered system has been discussed. Cyclic strain-controlled triaxial tests to evaluate the dynamic properties and liquefaction potential of Ahmedabad sands have been carried out. It has been brought out that the material immediately beneath the foundation plays a dominant role in controlling the dynamic response. Material at a depth greater than twice the width of the foundation plays an insignificant role. A major reduction in the shear modulus and a corresponding increase in the damping of Ahmedabad sand occur in the large shear strain range. As the initial densities of sand increase, the shear modulus shows clearly an increasing trend. However, more or less the same values of shear modulus occur beyond 0.5% shear strain level irrespective of their initial density. As a result of application of cyclic loads on the soils, pore water pressure builds up steadily and reaches initially applied confining pressure depending on the magnitude of cyclic shear strain as well as the density of the soil. At

higher cyclic shear strain amplitudes, the pore water pressure builds up fast and there is triggering of liquefaction at lower cycles. An increase in the density results in an increase in the cyclic strength of the soil there by making it less susceptible to liquefaction. The amplitude of cyclic shear strain governs the liquefaction resistance of a soil characterized by the cyclic strain approach.

- Bhandari, N. and Sharma, B. K., Damage pattern due to January, 2001 Bhuj earthquake, India: Importance of site amplification and interference of shear waves, Abstracts of International Conference on Seismic Hazard, New Delhi, 2001, pp. 19–21.
- Kramer, S. L., *Geotechnical Earthquake Engineering*, Prentice Hall, New Jersey, 1996.
- Ishihara, K., *Soil Behaviour in Earthquake Geotechnics*, Oxford University Press, New York, 1996.
- Skoglund, G. R., Marcuson, H. F. and Cunney, R. W., Evolution of resonant column test devices. *J. Geotech. Eng. ASCE*, 1976, **102**, 1147–1158.
- Sridharan, A. and Gandhi, N. S. V. V. S. J., Dynamic stiffness of soils. Proceedings of the International Conference on SM and FE, San Francisco, 1985, vol. 1, pp. 669–672.
- Fry, Z. B., Development and evaluation of soil bearing capacity, foundations structures, US Army Waterways experiment station, 1963, Tech. Report No. 3-632.
- Chae, Y. S., Vibrations of noncircular foundations. *ASCE J. of SM and FE div.* 95, 1969, SM6, 1411–1428.
- Sridharan, A. and Gandhi, N. S. V. V. S. J., Dynamic stiffness of soils. Proceedings of the Indian Geotechnical Conference, 1985, vol. 1, pp. 359–364.
- Gandhi, N. S. V. V. S. J., Studies on the shear modulus and damping factor of uniform and layered soils. Ph D thesis, IISc, Bangalore, 1986.
- Sridharan, A., Gandhi, N. S. V. V. S. J. and Suresh, S., Stiffness coefficients of layered soil system. *J. Geotech. Eng., ASCE*, 1990, **116**, 605–629.
- Odemark, N., Investigations as to the elastic properties of soils and design of pavements according to the theory of elasticity. Meddelande No. 77 Stateus vaginstut, Stockholm, 1949.
- Seed, H. B., Tokimatsu, K. and Harder, L. F., Influence of SPT procedures in soil liquefaction resistance evaluations. *J. Geotech. Eng., ASCE*, 1985, **111**, 1425–1445.
- Stark and Olson, S. M., Liquefaction resistance using CPT and field case histories. *J. Geotech. Eng., ASCE*, 1995, **121**, 856–869.
- Andrus, R. D. and Stokoe, K. H. Liquefaction resistance of soils from shear wave velocity. *J. Geotech. Geoenviron. Eng.*, 2000, **126**, 1015–1025.
- Xenaki, V. C. and Athanasopoulos, G. A., Liquefaction resistance of sand-mixtures: an experimental investigation of the effect of fines. *Soil Dyn. Earthquake Eng.*, 2003, 183–194.
- Lade, P. V. and Yamamuro, J. A., Effects of non-plastic fines on static liquefaction of sands. *Can. Geotech. J.*, 1997, **34**, 918–928.
- ASTM Designation: D 3999-91 (Reproduced 1996), Standard Test Methods for the Determination of the Modulus and Damping Properties of Soils using the Cyclic Triaxial Apparatus, Annual Book of ASTM Standards, 1996, vol. 04.08.
- Rollins, M. K., Evans, D. M., Diehl, B. N. and Daily III, W. D., Shear modulus and damping relationships for gravels. *Geotech. Geoenviron. Eng.*, 1998, 396–405.

ACKNOWLEDGEMENT. We thank the Department of Science & Technology, Government of India for financial support for the project 'In situ evaluation of soil liquefaction potential' under the grant No. DST/23/(287)/SU/2001.